

Theory of excitons in short-period superlattices

D. M. Whittaker

Royal Signals and Radar Establishment, St Andrews Road, Great Malvern, Worcestershire, WR14 3PS, United Kingdom

(Received 28 July 1989)

The exciton Hamiltonian for a superlattice is derived using an envelope-function-type description on the scale of the period of the structure. The solutions obtained include new exciton states which may have considerable oscillator strength and correspond to the electron and hole located in separate periods. The effects of applied electric and magnetic fields along the growth axis are considered. In an electric field there can be a large blue shift of the main exciton strength as the miniband decouples into a Stark ladder. In a magnetic field, the new exciton states evolve into extra series of Landau levels not observable in isolated quantum wells.

The full exciton Hamiltonian for a superlattice (SL) is difficult to solve exactly since it involves three nonseparable degrees of freedom: the axial coordinates of both electron and hole and their separation in the plane. Chomette *et al.*¹ have obtained variational solutions for the ground state, but this approach has limited application to higher states and is not easily adapted to the consideration of external fields. The problem can be simplified since in a SL with a period short enough to have a miniband (MB) width comparable to the exciton binding energy, the MB separation is typically much larger than this energy. Hence, to a good approximation, the exciton states can be derived from a reduced basis set corresponding to just one electron and one hole MB. This approach is similar to that of Chu and Chang,² who obtained approximate solutions to the integral equation [Eq. (3) of this paper], but the present method is also applicable to the treatment of external fields and gives accurate descriptions of the bound states.

The optically active exciton is constructed from states with total momentum $\mathbf{K} = 0$:

$$\Phi(\mathbf{k}, q; \mathbf{r}, n, \hat{z}_e, \hat{z}_h) = e^{i\mathbf{k}\cdot\mathbf{r}} e^{iqnd} f_e(\hat{z}_e) f_h(\hat{z}_h),$$

where \mathbf{k} is the in-plane momentum, \mathbf{r} the corresponding spatial separation, q the axial momentum, and nd (n integer, d the SL period) the axial separation of the electron and hole. $f_e(\hat{z}_e)$ and $f_h(\hat{z}_h)$ are the superlattice periodic envelope functions, with \hat{z}_e and \hat{z}_h ranging over only a single period. As in the development of the envelope-function theory for bulk semiconductors, it is necessary to neglect the q and \mathbf{k} dependence of f_e and f_h , but this should not be important provided the energy range of the states making up the exciton is small compared to the MB binding energies relative to the top of the barriers.

The Coulomb interaction mixes the basis states with matrix elements

$$\langle q' \mathbf{k}' | V | q \mathbf{k} \rangle = \sum_n \int d^2\mathbf{r} V_n(\mathbf{r}) e^{i(\mathbf{k}-\mathbf{k}')\cdot\mathbf{r}} e^{i(q-q')nd}, \quad (1)$$

where

$$V_n(r) = -\frac{1}{\epsilon_r} \int \int d\hat{z}_e d\hat{z}_h \frac{|f_e(\hat{z}_e)|^2 |f_h(\hat{z}_h)|^2}{[r^2 + (\hat{z}_e - \hat{z}_h + nd)^2]^{1/2}}. \quad (2)$$

The effective Schrödinger equation for the exciton envelope wave function can be written in integral form as (in atomic units)

$$\left[-\frac{k^2}{2\mu_t} + \epsilon(q) \right] \tilde{\psi}(q, \mathbf{k}) + \int_{-\pi/d}^{\pi/d} \frac{dq'}{2\pi} \int \frac{d^2\mathbf{k}'}{(2\pi)^2} \langle q' \mathbf{k}' | V | q \mathbf{k} \rangle \tilde{\psi}(q', \mathbf{k}') = E \tilde{\psi}(q, \mathbf{k}), \quad (3)$$

where $\epsilon(q)$ is the SL MB dispersion and μ_t the in-plane reduced mass.

As the matrix element depends only on $q - q'$ and $\mathbf{k} - \mathbf{k}'$, the potential-energy term is just a convolution of the Fourier transform of $V_n(r)$ with $\tilde{\psi}(q, \mathbf{k})$. Thus, the Schrödinger equation transforms into a differential equation:

$$-\frac{1}{2\mu_t} \nabla_r^2 \psi(n, \mathbf{r}) + \frac{1}{2\mu_t d^2} [2\psi(n, \mathbf{r}) - \psi(n+1, \mathbf{r}) - \psi(n-1, \mathbf{r})] + V_n(r) \psi(n, \mathbf{r}) = E \psi(n, \mathbf{r}). \quad (4)$$

The q variable is restricted to the range $\pm\pi/d$, so its Fourier transform leads to a discrete n space with separation d . Equation (4) corresponds physically to a single particle moving in a series of two-dimensional planes, one for each period of the SL, coupled by quantum-

mechanical tunneling. As written, only coupling between adjacent planes is included, usually a good approximation, but more distant terms can be added if necessary to fit $\epsilon(q)$. $V_n(r)$ is Coulombic at long range, but weakened for small n and r due to the averaging over \hat{z}_e and \hat{z}_h , so

there is only a logarithmic singularity as $r \rightarrow 0$ on $n=0$. In the isolated quantum-well limit, $d \rightarrow \infty$, there is no coupling between the planes, and the result is identical to the effective-potential theory which has been used to describe the quantum-well exciton.^{3,4} An equivalent discrete Hamiltonian and modified potential is obtained in the usual envelope-function theory for bulk semiconductors, but in that case the periodicity is that of the lattice, which is much smaller than the exciton, so the result can be approximated by a continuum with a Coulomb interaction. Here, however, the exciton size is comparable to the period, so the discrete nature cannot be neglected.

Equation (4) is solved here by using a finite set of $2d$ exciton states in the uncoupled planes as a basis within which the coupling term is diagonalized. All the calculations have been carried out for GaAs-AlAs SL's with equal well and barrier widths. The hole masses are obtained from a zone center fit to solutions of a two-band Luttinger Hamiltonian calculation including coupling of light and heavy states.⁵ Electron masses and miniband parameters, which include coupling of up to next-nearest-neighbor planes, are fits to the dispersion obtained from Bastard's three-band Kane model⁶ of the light-particle band structure. The dielectric constant, ϵ_r , is an average of GaAs and AlAs parameters, weighted according to the single-particle probability densities for each material.

Figure 1 shows the binding energies and oscillator strengths of some of the lower exciton states as the SL period, measured in monolayers (1 ML ≈ 2.83 Å), is reduced and the MB width (dashed line and right-hand scale) increases. The numbers on the curves indicate the uncoupled states which make the largest contribution to the wave function: the first of each pair is the axial separation $|n|$ in periods and the second the in-plane radial quantum number n_r . They provide a reasonable description of the state for the case of weak coupling between wells, though, as in the case of the anisotropic three-dimensional exciton, there are no good quantum numbers. At stronger coupling, the notation becomes increasingly inexact, with several basis states generally making comparable contributions to each exciton state.

For MB widths smaller than or similar to the exciton binding energy, the major effect of the coupling is to give oscillator strength to the axially separated finite n states, not seen in the isolated well. The strength of these transitions increases with miniband width, reaching $\sim 10\%$ of the ground-state oscillator strength. As the coupling increases further, all the states spread out both axially and radially, as indicated by the increasing n labels on the initially (1,0) state, becoming weaker and less-tightly bound. This effect may be considerable: the MB width increases roughly exponentially with decreasing period, so μ_i can become very small, leading to very weak excitonic features.

A uniform axial electric field F is represented by a term $F(z_e - z_h)$ in the full SL Hamiltonian. This can be approximated in the effective Hamiltonian as Fnd , provided there is no quantum-confined Stark effect, i.e., the field is weak enough to leave the SL envelope functions $f_e(\hat{z}_e)$ and $f_h(\hat{z}_h)$ unmodified. This requires the potential drop

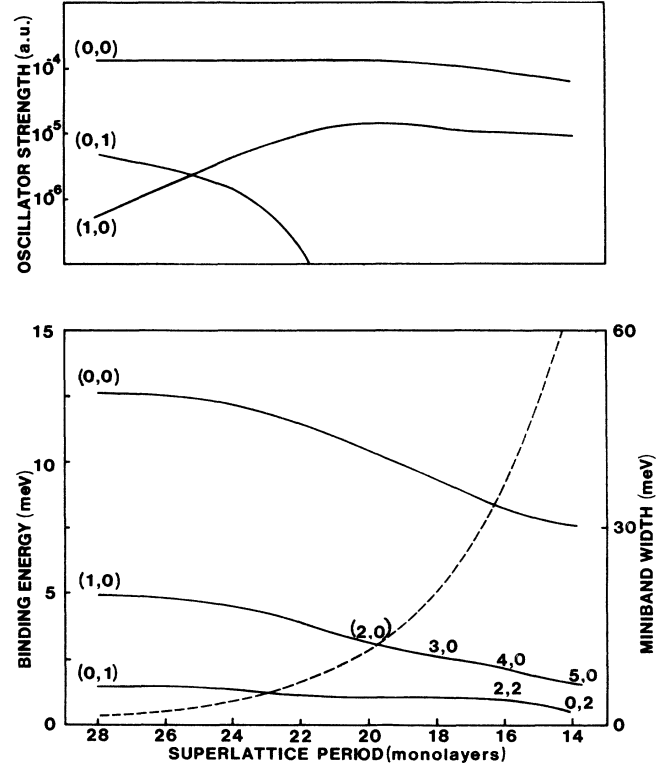


FIG. 1. Binding energies and oscillator strengths of the stronger exciton states in a GaAs-AlAs SL as a function of the period in units of monolayers. The dashed line and right-hand scale show the variation of the MB width. (n, n_r) labels on the curves indicate the basis state which gives the largest contribution to the wave function (see text). Weak anticrossings between the (0,1) state and higher n ($n, 0$) states (not plotted) are omitted for clarity. The figure shows the transition from quasi- $2d$ to anisotropic- $3d$ excitons, characterized by a general reduction in binding energies and the strengthening of the axially separated (1,0) state.

across a single well to be small compared with the MB separation, a condition satisfied in fields up to fields $\sim 10^5$ V cm⁻¹ in the structures considered here.

In the electric field, all the states are resonances: a "bound" state in a given well always mixes with continuum states of similar energy from further along the SL, which tends to broaden and weaken the peaks in regions of the spectrum where the background is large. This effect is not accounted for in the present solution, since the basis does not include continuum states, so the oscillator strengths obtained for positive n states will not accurately reflect their spectral strength.

The effect of the field on the energies and intensities of some of the bound states in the 14-ML-period SL is shown in Fig. 2. At high fields, the wells uncouple to give a Stark ladder of $2d$ exciton states well localized in individual periods, with all the $n \neq 0$ transitions losing strength rapidly as the field increases. The (n, n_r) labels are, in this limit, exact quantum numbers and will be used to label the states, although at lower fields they are not even approximate descriptions of the wave functions.

The excitons are bound by their $2d$ binding energies relative to a value Fnd above the center of the MB. Hence, the main spectral peak undergoes a large blue shift, of half the MB width minus the difference between the isolated well and SL binding energies. In the process, its oscillator strength increases by a factor of ~ 2 due to the increased localization. The $n = \pm 1$ states are less tightly bound, so appear asymmetrically placed with respect to the $n = 0$ peak.

At lower fields, this description breaks down because of the strong mixing of the states due to the coupling term. The energies are shifted and anticrossings occur, with the result that there are very significant exchanges of oscillator strength as the field is varied. The plot of the oscillator strengths shows how the strongest peak passes to suc-

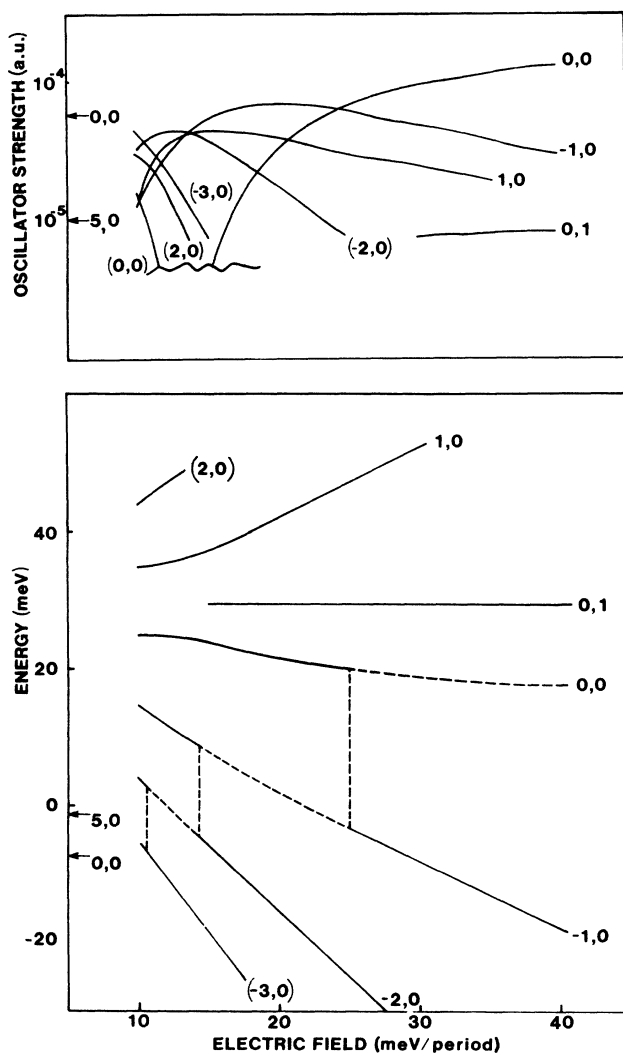


FIG. 2. Evolution of the energies and oscillator strengths of some of the exciton states of the 14-ML-period SL in an axial electric field, the arrows indicating zero-field values. Weaker anticrossings are again omitted for clarity. The zero of energy is the bottom of the MB. The strongest spectral peak shifts from state to state, as indicated by the dashed line, giving a blue shift of approximately half the MB width when the field decouples the wells.

cessively lower states when the field is reduced, as indicated by the dashed lines superimposed on the energy curves. The subsidiary $n \neq 0$ peaks move between states in a similar way, so the strength in each state oscillates with the field, although for the relatively narrow bandwidth used here only the first minimum of the $(0,0)$ state can be seen in the range of fields shown. These oscillations are similar to those predicted on the basis of a single-particle picture,⁷⁻¹¹ but their form is modified by the excitonic effects.

An axial magnetic field can easily be incorporated in the solution, since it alters only the in-plane motion, via the diamagnetic confinement term $\frac{1}{32}\mu^3\epsilon_r^{-4}\gamma^2r^2$, where γ is the cyclotron energy in rydbergs. The calculation proceeds as before, except the uncoupled basis states become two-dimensional magnetoexcitons. There is no further approximation in this treatment, so the only restriction is that the separation of the Landau level from those of the next MB must be large compared with the exciton binding energy.

The effect of the magnetic field on the energies and intensities of some of the bound states in the 20-ML SL is shown in Fig. 3. The field separates states according to their in-plane extent, so at high field n_r is a good quantum number, and the states are grouped in Landau levels

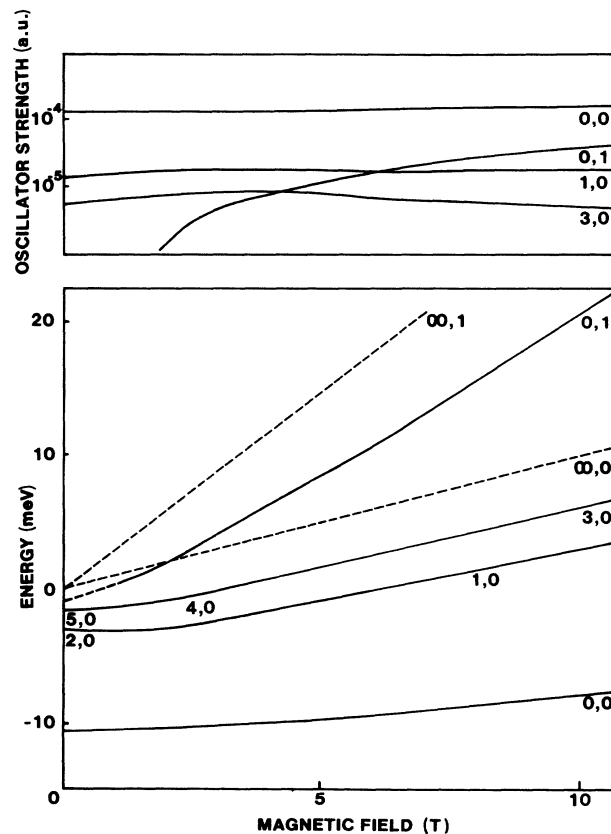


FIG. 3. Evolution of the energies and oscillator strengths of some of the exciton states of the 20-ML-period SL in an axial magnetic field. The zero of energy is the bottom of the MB. The dashed lines (∞, n_r) are Landau levels. At high fields, the axially separated exciton states give rise to distinct sets of Landau levels with significant oscillator strength.

at energies approximately $(n_r + \frac{1}{2})\gamma$. However, the axial motion is not constrained by the field, so a series of one-dimensional bound and continuum exciton states are associated with each Landau level. As the field is raised, the radial confinement increases, so the exciton binding becomes stronger and its axial extent smaller. The width of the one-dimensional continuum is only the MB width, so the one-dimensional exciton is dominated by the lowest line, and as the field increases, its oscillator strength grows at the expense of the rest. However, the first excited states should be resolvable at high fields and will take the form of a second set of Landau levels lying between the main $(0, n_r)$ peaks. This second structure has significant oscillator strength, and the energy separations from the corresponding $(0, n_r)$ levels are only weakly field dependent.

There have been numerous determinations of exciton binding energies¹²⁻¹⁶ in SL's. Although none correspond precisely to the structures discussed here, the trend for weaker, more loosely bound exciton ground states at large MB widths seems to be established. Structure above the main exciton peak has also been observed^{9,12,13,15} and has variously been attributed to the continuum edge, $2s$ state, or a saddle-point resonance associated with the M_1 singularity at the top of the miniband. The clearest results are those of Deveaud *et al.*,¹³

who observe a strong ($\sim 5\%$) peak about 8 meV above the main exciton line in a SL with MB width ~ 10 meV. This is in good agreement with the values calculated here for the axially separated $(1,0)$ state in a comparable structure, and the behavior observed in a magnetic field is similar to that predicted, with the peak evolving into one of a separate set of Landau levels. The authors attribute this peak to a saddle-point resonance, but calculations¹⁷ suggest that the MB width is insufficient to support a resonance of the required strength.

Stark ladders have been observed at high electric fields in many structures,^{8,9,15,16,18} with n up to ± 6 .⁸ Only $n_r=0$ states are reported, but this is not surprising considering that the finite n_r states are as weak as those in an isolated well. The behavior seems to be qualitatively similar to that predicted here, with large blue shifts of the main exciton feature observed in structures with sufficient bandwidth.^{7,18} The asymmetry in the energies of the $n=0, \pm 1$ peaks is evident^{9,18} as are the general features of the field dependence of energies and oscillator strengths depicted in Fig. 2.

The author wishes to thank M. S. Skolnick and K. J. Nash of the Royal Signals and Radar Establishment (RSRE) for various helpful discussions and their critical reading of the manuscript.

¹A. Chomette, B. Lambert, B. Deveaud, F. Clerot, A. Regreny, and G. Bastard, *Europhys. Lett.* **4**, 461 (1987).

²H. Y. Chu and Y.-C. Chang, *Phys. Rev. B* **36**, 2946 (1987).

³G. Duggan, *Phys. Rev. B* **37**, 2759 (1988).

⁴D. M. Whittaker and R. J. Elliott, *Solid State Commun.* **69**, 1 (1988).

⁵M. Altarelli, U. Ekenberg, and A. Fasolino, *Phys. Rev. B* **32**, 5138 (1988).

⁶G. Bastard, *Superlatt. Microstruct.* **1**, 256 (1985).

⁷J. Bleuse, G. Bastard, and P. Voisin, *Phys. Rev. Lett.* **60**, 220 (1988).

⁸J. Barrau, K. Khirouni, Do Xuan Than, T. Amand, and M. Brousseau, *Topical Meeting on Quantum Wells for Optics and Optoelectronics*, Vol. 10 of 1989 *Technical Digest Series* (Optical Society of America, Washington, D.C., 1989), p. 6.

⁹J. Bleuse, P. Voisin, M. Allovon, and M. Quilicq, *Appl. Phys. Lett.* **53**, 2632 (1988).

¹⁰D. Emin and C. F. Hart, *Phys. Rev. B* **36**, 7353 (1987).

¹¹B. Jogai and K. L. Wang, *Phys. Rev. B* **35**, 653 (1987).

¹²A. Chomette, B. Deveaud, M. Baudet, P. Auvray, and A. Regreny, *J. Appl. Phys.* **59**, 3835 (1986).

¹³B. Deveaud, A. Regreny, M. Baudet, A. Chomette, J. C. Maan, and R. Romestain, in *Proceedings of the Eighteenth International Conference on the Physics of Semiconductors, Stockholm, Sweden, 1986*, edited by O. Engström (World Scientific, Singapore, 1987), p. 695.

¹⁴K. J. Moore, G. Duggan, P. Dawson, C. T. Foxon, N. J. Pufford, and R. J. Nicholas, *Phys. Rev. B* **39**, 1219 (1989).

¹⁵P. Voisin, J. Bleuse, C. Bouche, S. Gaillard, C. Alibert, and A. Regreny, *Phys. Rev. Lett.* **61**, 1639 (1988).

¹⁶R. H. Yan, R. J. Simes, H. Ribot, L. A. Coldren, and A. C. Gossard, *Appl. Phys. Lett.* **54**, 1549 (1989).

¹⁷D. M. Whittaker (unpublished).

¹⁸E. E. Mendez, F. Agulló-Rueda, and J. M. Hong, *Phys. Rev. Lett.* **60**, 2426 (1988).